(ANPA Conference 2024)
ISSN: 2392-473X(Print), 2738-9537 (Online)

Research Article ©Nepal Physical Society
DOI: https://doi.org/10.3126/jnphyssoc.v10i1.72845

Comparative Analysis of Different Models within RadEst 3.0 for Solar Radiation Estimation at Dhankutta, Nepal

Basanta Kumar Rajbanshi,[1, a)] Ram Gopal Singh,[1, b)] Bed Raj KC,[2, c)] and Khem Narayan Poudel[3, d)]

[1)] *Department of Physical Sciences, Shri Ramswaroop Memorial University (SRMU), Lucknow, India*
[2)] *Mahendra Multiple Campus, Tribhuvan University, Nepalgunj, Nepal*
[3)] *Department of Applied Sciences, Pulchowk Campus, IOE, TU, Patan, Nepal*

[a)] *Corresponding author: basantaraz22@gmail.com, basantaraz05@gmail.com*
[b)] *Electronic mail: dean.phy@srmu.ac.in*
[c)] *Electronic mail: bedrajkc@yahoo.com*
[d)] *Electronic mail: khem@ioe.edu.np*

Abstract. To develop efficient solar energy technologies, it is essential to understand accurately the distribution of solar radiation in each geographical location. This research project estimates total solar radiation reaching a surface daily in Dhankutta (26.983°N, 87.346°E, 1192 m), Nepal by utilizing weather data including temperature, humidity, wind speed, rainfall, and measured solar radiation data. Four distinct models (Bristow-Campbell (BC), Campbell-Donatelli (CD), Donatelli-Bellocchi (DB), and Donatelli-Campbell-Bristow-Bellocchi (DCBB)) were employed to estimate global solar radiation (GSR). Root mean square error (RMSE), coefficient of residual mass (CRM), mean bias error (MBE), mean percentage error (MPE), and coefficient of determination (R^2) were among the statistical tools used to assess the effectiveness of models. By minimizing RMSE, and CRM, and maximizing R^2, parameter fitting (PF) is used to calibrate all four models. The annual mean daily GSR for 2021 and 2022 was determined to be 14.5 ± 0.25 MJ/m²/day and 15.7 ± 0.24 MJ/m²/day, respectively, indicating sufficient potential for solar energy generation. The maximum GSR of 37.6 MJ/m^2/day and 26.5 MJ/m^2/day were observed in 2021 and 2022 respectively. Among the four models used to estimate GSR, the CD model showed the highest accuracy with an R^2 value of 0.60 so the CD model is considered the most reliable method for predicting GSR levels in this area.

Received: August 25, 2024; **Revised**: October 10, 2024; **Accepted**: October 23, 2024

Keywords: pyranometer, statistical tools, meteorological factors, GSR, climate transmissivity, RadEst 3.0 programme.

1. INTRODUCTION

On the global map, Nepal is in the solar energy-friendly range. It is located between longitude 80°4'- 88°12' E and latitude 26°22' - 30°27' N. However, the lack of fossil fuels causes severe energy problems, holding back its development. Solar radiation is a secure and clean energy source. An average of 3.6 to 6.2 kWh/m^2/day of solar insolation occurs annually in the country. Nepal has 300 sunny days and 6.8 hours of sunshine each year, indicating a large potential for free and clean solar energy.[1]

Ali, M. A. et al. explored using artificial neural networks to improve the accuracy of global sun radiation predictions compared to traditional methods.[2] Teyabeen, A. et al. utilized these advancements to calculate monthly global sun radiation levels across twelve major cities of Libya.[3]. Building upon this, Narejo K A et al. computed global, beam, and diffuse solar radiation for five major cities worldwide: Karachi, Tokyo, New York, London, and Sydney.[4]

The current annual average GSR of the nation is 4.23 kWh/m^2/day.[5] Therefore, in developing Asian nations like Nepal, solar energy is one of the finest solutions to the energy crisis.[6] Joshi et al. estimated GSR for Khumaltar and estimated GSR for Kathmandu, Nepal, using several empirical models.[7]. For Biratnagar, Nepal, Dhakal et al. investigated various empirical models based on temperature, artificial neural networks, and machine learning models for estimating GSR.[8] Joshi et al. estimated daily GSR at Western Highland, Simikot, Nepal using RadEst 3.0 software.[9] Poudyal et al. used the RadEst 3.0 software to calculate the GSR for Kathmandu, Nepal, based on data from 2005 and 2007.[10]. Similarly, at Simara Airport in Nepal, they calculated the GSR.[11] Chhetri and Gurung analyzed data from 2011 and 2013 in Jumla, Nepal, to calculate GSR using the RadEst 3.00 software.[12]

This study is motivated by the urgent need to harness

solar energy in Nepal, where abundant solar resources remain underutilized. Understanding the precise distribution of solar radiation is critical for optimizing solar energy technologies and informing energy policy. The authors employed a systematic approach that integrated local weather data with advanced modeling techniques to assess GSR accurately. By comparing multiple models, this research identifies the most effective method for estimating solar radiation in Dhankutta and enhances the understanding of solar energy potential in diverse geographical contexts. This work adds significant value by providing empirical data and methodological insights that can guide future solar energy projects and contribute to sustainable energy development in the region.

2. RadEst3.0 SOFTWARE

Estimating daily GSR is important to advance solar energy research. The study aims to identify optimal methods for calculating daily GSR in Nepal. We evaluate the performance of RadEst 3.0 software, which utilizes readily available meteorological data like temperature, humidity, wind speed, and precipitation to estimate GSR. This user-friendly software offers a valuable tool for future solar energy research in similar geographic regions.

Models

Four models; DCBB, BC, CD, and DB were used to estimate daily solar radiation. These models calculate results using statistical methods and specific parameters.

Estimated transmissivity (tt_i), clear sky transmissivity (τ), monthly average temperature (ΔT), daily maximum air temperature (T_{max}), daily minimum air temperature (T_{min}), coefficient of temperature range (b), very sensitive empirical parameter (c), temperature factor (T_{nc}), seasonal variation magnitude parameter (c_1), seasonal variation profile parameter(c_2), day of the year (i = 1 to 365 or 366), average temperature function $\{f(T_{avg})\}$, minimum temperature function $\{f(T_{min})\}$, estimated radiation {Est Rad_i in (MJ m^{-2} day^{-1})}, potential radiation outside the atmosphere {$PotRad_i$) in (MJ m^{-2} day^{-1})}

These models calculate the atmospheric transmissivity of solar radiation using the difference between the maximum and minimum air temperatures. The estimated value of radiation (Est Rad_i) is the product of the estimated transmissivity (tt_i) and the value of potential radiation (Pot Rad_i) outside the earth's atmosphere.

Est Rad_i = tt_i Pot Rad_i

$$PotRed_{doy} = 117.5 dd_2 \frac{h_s Sin(lat)\ Sin(dec) + Cos(lat)\ Sin(h_s)}{\pi} \quad (1)$$

In this equation, lat means the latitude of the monitoring site, measured in degrees, dec is solar declination, dd_2 is the sun's distance, and h_s is half-day length.

2.1 BC Model[13]

The BC model, the foundation of subsequent models, estimates daily solar radiation using the relationship between air temperature range and solar radiation. This model assumes that cloud cover affects both maximum and minimum temperatures, and that clear skies lead to higher temperatures. Estimated transmissivity is,

$$tt_i = \tau \left[1 - exp\left(\frac{-b\ \Delta T_i^c}{month\ \Delta T}\right)\right] \quad (2)$$

Hence from the equation, the estimated radiation provided is given by,

$$Est\ Red_i = \tau \left[1 - exp\left(\frac{-b\ \Delta T_i^c}{month\ \Delta T}\right)\right] PotRed_i \quad (3)$$

Where,

$$\Delta T_i = T_{max_i} - \frac{T_{min_i} + T_{min(i+j)}}{2} \quad (4)$$

2.2 CD Model[14]

The CD is derived from the modification of the BC model. In this model, transitivity is obtained as

$$tt_i = \tau \left[1 - exp\ \left\{-b \times f\ (T_{avg})\ \Delta T_i^2\ f(T_{\min})\right\}\right] \quad (5)$$

Thus,

Est Red_i =

$$\tau \left[1 - exp\ \left\{-b \times f\ (T_{avg})\ \Delta T_i^2\ f_1(T_{\min})\ PotRed_i\right\}\right] \quad (6)$$

Where,

$$T_{avg} = \frac{T_{max_i} + T_{min_i}}{2} \quad (7)$$

2.3 DB Model[15, 16]

DB model is the third model. It estimates total solar energy from air temperature, integrating variations in clear sky transmissivity and using seasonality factors (c_1, c_2) to calculate temperature differences. The transmissivity in the DB model is obtained as,

$$tt_i = \tau \left[1 + f(i)\left[1 - exp\left\{\frac{-b\ \Delta T^2}{\Delta T_{week}}\right\}\right]\right] \quad (8)$$

Providing radiation estimates as,

$EstRed_i$ =

$$\tau \left[1 + f(i)\left[1 - exp\left\{\frac{-b\ \Delta T_i^2}{\Delta T_{week}}\right\}\right]\right] PotRed_i \quad (9)$$

Where,

$$f(i) = c_1 \left[\sin\left(i\, c_2 \frac{\pi}{180}\right) + cos\left\{i\, f(c_2) \frac{\pi}{180}\right\}\right] \quad (10)$$

$$f(c_2) = 1 - 1.90\, c_3 + 3.83 c_3^2 \quad (11)$$

$$c_3 = c_2 \text{ integer } (c_2) \quad (12)$$

2.4 DCBB Model[13, 14, 15, 16]

The DCBB model is a versatile model incorporating features from the previous three. By adjusting parameters, users can switch between models. For example, setting c_1 to zero and selecting the average monthly ΔT option transforms the DCBB model into the BC model. The estimated transmissivity is,

$$tt_i = \tau \left[1 + f(i)\left[1 - exp\left\{\frac{-b\ \Delta T^2 f(T_{\min})}{\Delta T_{avg}}\right\}\right]\right] \quad (13)$$

Which provides radiation estimates as,

$EstRed_i$ =

$$\tau \left[1 + f(i)\left[1 - exp\left\{\frac{-b\ \Delta T_i^2 f(T_{\min})}{\Delta T_{avg}}\right\}\right]\right] PotRed_i \quad (14)$$

Where,

$$f(i) = c_1 \left[\sin\left(i\, c_2 \frac{\pi}{180}\right) + cos\left\{i\, f(c_2) \frac{\pi}{180}\right\}\right]$$

$$f(c_2) = 1 - 1.90\, c_3 + 3.83 c_3^2$$

$$f(T_{avg}) = 0.017 exp\ \left\{\ exp\ (-0.053 \times T_{avg})\right\} \quad (15)$$

Where,

$$T_{avg} = \frac{T_{max_i} + T_{min_i}}{2}$$

$$f(T_{\min}) = exp \frac{T_{\min}}{T_{nc}} \quad (16)$$

$c_3 = c_2$ integer (c_2)

3. METHODS AND INSTRUMENTATION

3.1 Site Selection

Dhankutta (26.983°N, 87.346°E), a town situated at 1192 meters, experiences a generally warm and pleas-

Table 1: GSR values (average, maximum, annual total) were measured and modeled for Dhankutta in 2021

Model	Average GSR (MJ/m^2/day)			Maximum GSR (MJ/m^2/day)			Total GSR (MJ/m^2)		
	AO	Mea	PF	AO	Mea	PF	AO	Mea	PF
BC	14.3	14.5	15.6	24.1	37.6	25.1	5236	5303	5686
CD	15.5	14.5	15.4	24.8	37.6	24.8	5646	5303	5619
DB	14.3	14.5	15.6	21.8	37.6	22.8	5203	5303	5676
DCBB	13.6	14.5	15.5	21.5	37.6	22.8	4947	5303	5673

Table 2: GSR values (average, maximum, annual total) were measured and modeled for Dhankutta in 2022

Model	Average GSR (MJ/m^2/day)			Maximum GSR (MJ/m^2/day)			Total GSR (MJ/m^2)		
	AO	Mea	PF	AO	Mea	PF	AO	Mea	PF
BC	15.5	15.7	15.7	25.2	26.5	25.3	5661	5734	5727
CD	15.6	15.7	15.7	24.8	26.5	24.9	5694	5734	5729
DB	15.4	15.7	15.7	23.8	26.5	24.1	5616	5734	5729
DCBB	14.7	15.7	15.7	22.4	26.5	23.3	5360	5734	5733

ant climate and receives significantly less rainfall during winter than summer.

3.2 Instrument

Weather data, including solar radiation, maximum and minimum temperature, rainfall, maximum and minimum humidity, and wind speed, served as inputs for the models. This information was collected by the Department of Hydrology and Meteorology, Government of Nepal (GoN) for Dhankutta during 2021 and 2022. Rainfall was measured using a rain gauge (udometer), while temperature was recorded with a maximum-minimum thermometer. Sunlight levels were captured by a CMP6 Pyranometer, which operates based on thermocouple technology and can measure a broad range of light wavelengths under various temperature conditions. [17]

3.3 File Format

The data for the study was stored in a simple text format (ASCII) without any labels at the beginning. Each line of this file contained eight pieces of information separated by spaces.

3.4 Input Format

To start, the RadEst 3.00 software requires the specific latitude, longitude, and elevation of a location. Additionally, a clear sky transmissivity value between 0.6 and 0.8 must be provided.

3.5 Analysis

After inputting location details (latitude, longitude, altitude), data is accessed from an ASCII file. Two methods, parameter fitting (PF) and auto-optimization (AO) are applied to different models. PF is more precise than AO. Both methods require at least two years of data for comparison and solar radiation calculations. PF involves adjusting model parameters to match observed and estimated radiation values, which are then compared graphically. The models generate various statistical metrics like RMSE, CRM, correlation coefficient, R², MBE, MPE, ME, and CV to evaluate their performance.

4. RESULTS AND DISCUSSION

All models were initially tested using auto-optimization, but the results were deviated. Subsequently, parameter fitting was applied to 2022 data to optimize the models. Table 2 compares model outputs (average, maximum, and annual total GSR) for both methods. The average annual GSR was found to be 15.7 MJ/m^2/day. Using 2022 model parameters, GSR for 2021 was estimated with minimal error. Table 1 shows these results. Compared to other models, the CD model demonstrated superior accuracy for both 2021 and 2022, as indicated by closer agreement between measured and estimated GSR values (average, maximum, and total). Thus, the CD model is recommended for GSR estimation in hilly regions during these years.

Figure 4 displays the seasonal changes in GSR for 2021 and 2022. Spring had the highest GSR levels (16.32 ± 0.54 MJ/m²/day in 2021, 17.88 ± 0.46 MJ/m²/day in 2022) due to clear skies after the rainy season. In contrast, winter experienced the lowest GSR (13.14 ± 0.27 MJ/m²/day in 2021, 13.46 ± 0.31 MJ/m²/day in 2022) caused by clouds and rain. Solar radiation peaks in spring and is lowest in winter due to humidity, cloud cover, rainfall, and wind. Maximum radiation occurs after the monsoon ends (June-August) when the skies clear.

Figure 5 illustrates the monthly changes in GSR for 2021 and 2022. GSR peaked in April 2021 (19.14 ± 0.71 MJ/m²/day) and May 2022 (18.97 ± 0.88 MJ/m²/day) due to clear post-rainy season skies. Conversely, GSR was lowest in January 2021 (12.78 ± 0.40 MJ/m²/day) and December 2022 (12.69 ± 0.19 MJ/m²/day) due to clouds and rain. Overall, GSR patterns remained consistent over the two years, with error bars indicating monthly variability.

Figure 6 depicts the seasonal rainfall patterns for 2021 and 2022. Summer 2021 experienced the highest rainfall (607.37 mm), while winter 2021 had the lowest

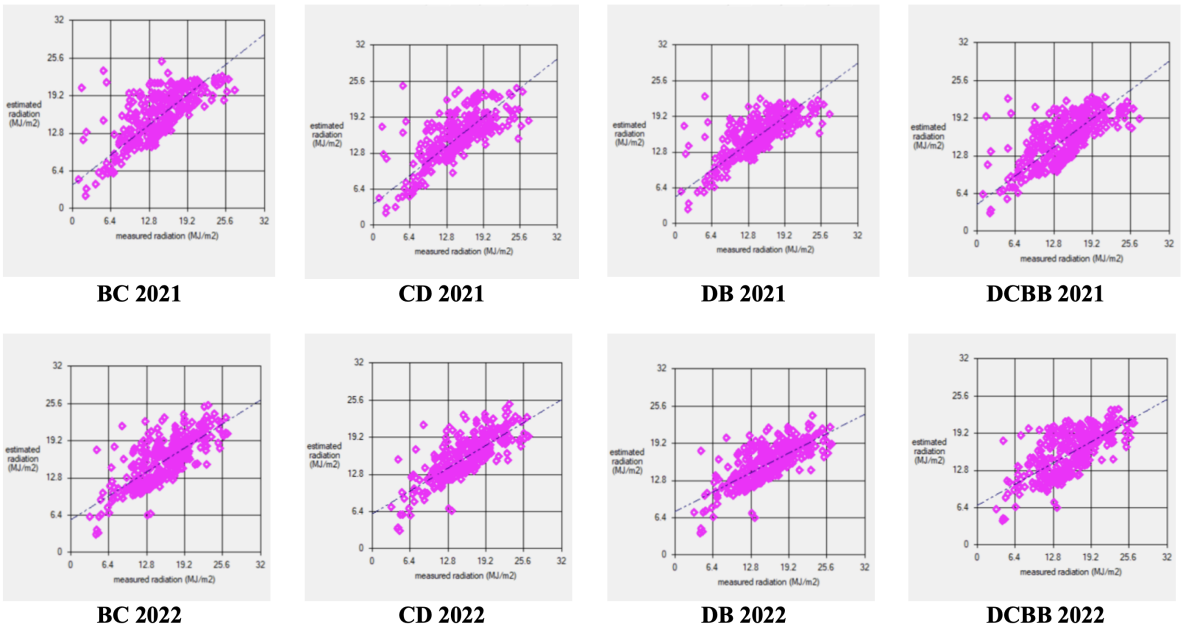

FIGURE 1: Linear correlation between measured and estimated GSR for 2021 and 2022

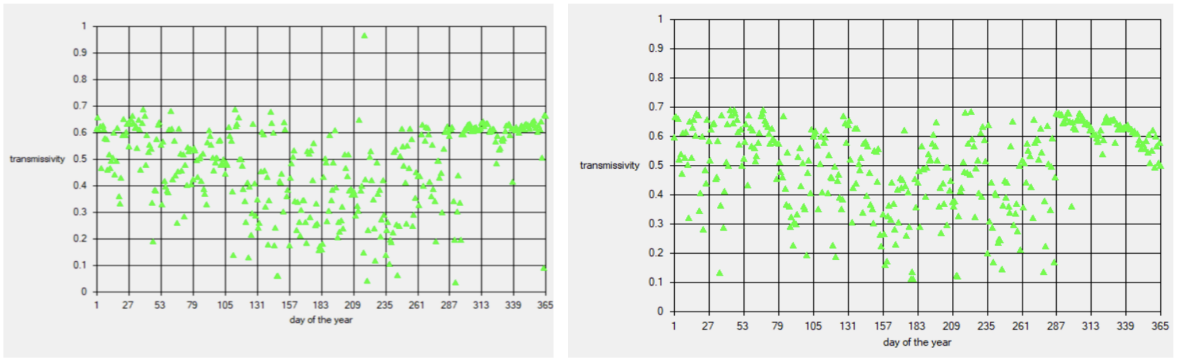

FIGURE 2: Daily change in atmospheric transmissivity at Dhankutta for 2021 and 2022

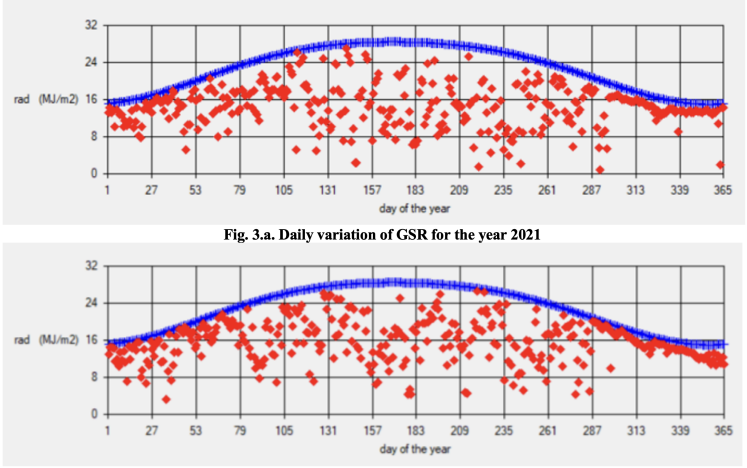

FIGURE 3: Daily GSR variation at Dhankutta for 2021 and 2022

Table 3 : Error analysis for Dhankutta in 2021

Model	MBE ($MJ/m^2/day$)	RMSE ($MJ/m^2/day$)	MPE (%)	r	CRM ($MJ/m^2/day$)	R^2	ME	CV
BC	1.12151	3.68	-18.498	0.80638	-0.07	0.48	0.40	25.30
CD	0.9463	3.60	8.64822	0.81379	-0.06	0.49	0.42	24.80
DB	1.1018	3.51	-19.149	0.81857	-0.07	0.50	0.45	24.19
DCBB	1.08733	3.77	-19.419	0.78965	-0.07	0.44	0.37	25.95

Table 4: Error analysis for Dhankutta in 2022

Model	MBE ($MJ/m^2/day$)	RMSE ($MJ/m^2/day$)	MPE (%)	r	CRM ($MJ/m^2/day$)	R^2	ME	CV
BC	-0.01784	3.09	-4.10217	0.741703	0.00	0.55	0.53	19.65
CD	-0.01408	2.86	-4.18725	0.774362	0.00	0.60	0.60	18.23
DB	-0.01378	3.10	-5.34358	0.728885	0.00	0.53	0.53	19.72
DCBB	-0.00290	3.37	-5.15748	0.684089	0.00	0.47	0.45	21.43

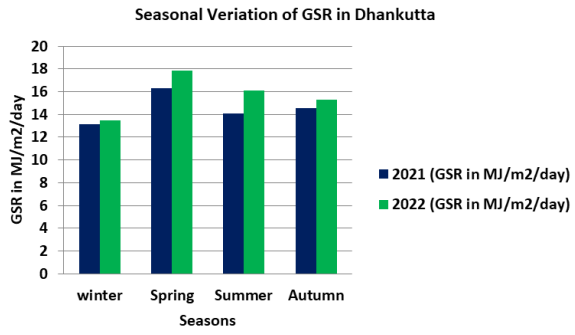

FIGURE 4: Seasonal variation of GSR at Dhankutta for 2021 and 2022

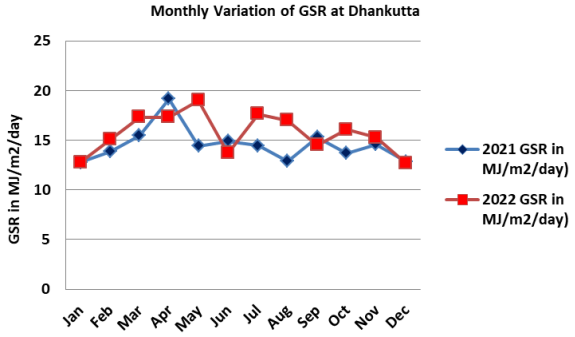

FIGURE 5: Monthly variation of GSR at Dhankutta for 2021 and 2022

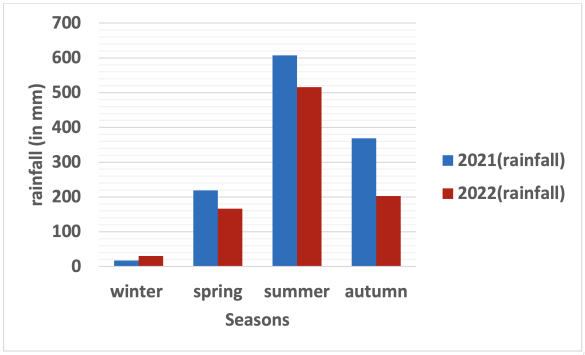

FIGURE 6: Seasonal variation of precipitation at Dhankutta for 2021 and 2022

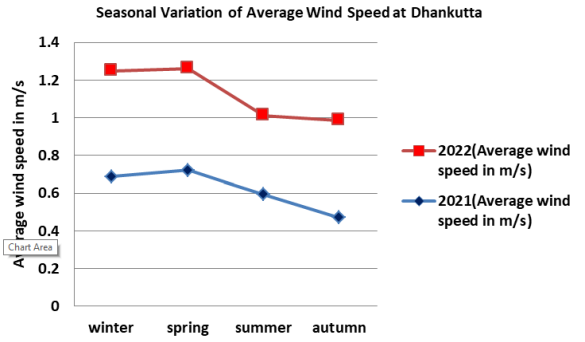

FIGURE 7: Seasonal variation of average wind speed at Dhankutta for 2021 and 2022

(17.5 mm). Figure 7 shows how average wind speed varied seasonally over the same period. Spring 2021 and 2022 recorded the highest wind speeds (0.725 m/s), whereas summer had the lowest (0.421 m/s).

The highest radiation levels occurred on April 6, 2021 (37.59 MJ/m²/day) and August 7, 2022 (26.45 MJ/m²/day), while the lowest occurred on October 19, 2021 (0.97 MJ/m²/day) and February 4, 2022 (3.29 MJ/m²/day). Temperature peaks were reached on September 10, 2021 (31.6°C) and July 15, 2022 (33.7°C), with lows of January 30, 2021 (6.0°C) and January 28, 2022 (4.8°C). Rainfall peaked on October 20, 2021 (163 mm) and September 1, 2022 (60.3 mm), while the highest wind speeds were recorded on December 26, 2021 (1.64 m/s) and December 26, 2022 (1.44 m/s).

4.1 Error Analysis

Tables 3 and 4 compare predicted and measured GSR accuracy for 2021 and 2022. The CD model showed the best overall performance as indicated by a higher R^2 value (0.60), with lower error values and a stronger correlation between predicted and measured data than other models. Fig. 1 shows strong agreement between

measured & estimated GSR for different models in 2021 & 2022, likely due to rainfall & regional climate. Figs. 2a & 2b show daily changed air transmittance after rain in both years. Figs. 3a & 3b indicate high GSR availability in Dhankutta, with low radiation & high transmittance despite a narrow zenith angle in winter.

Summer (June-August) has low GSR due to rain, clouds, and strong winds despite high temperatures. Post-rain clear skies lead to increased GSR in autumn. GSR generally rises from June to August and falls in December but is influenced by temperature and precipitation. Cloud cover and rain reduce GSR in summer. Precipitation negatively impacts GSR while temperature positively affects it.

Jumla, a mid-altitude region, receives more solar radiation (GSR) than Simikot, a high-altitude mountain area (6648 MJ/m² in 2013 and 7309 MJ/m² in 2011). The BC model is more accurate for Jumla than Simikot. Simikot has a higher GSR in spring and fall, while Jumla's peak GSR is in spring. These differences are due to altitude and local weather conditions. [12]

While Simikot, located at a higher altitude, might generally receive more sunlight, Jumla's higher recorded global solar radiation (GSR) is likely due to several factors. The clearer skies and less cloud cover in Jumla allow for more direct sunlight to reach the ground. Seasonal changes, especially during spring when the sun is most directly overhead, can also contribute to Jumla's higher GSR. The specific location and measurement techniques used could also play a role in the recorded data, emphasizing that solar radiation patterns can vary significantly between regions.

5. CONCLUSION

Analysis of Dhankutta's solar radiation data for 2021 and 2022 reveals average daily levels of 14.5 ± 0.25 MJ/m²/day and 15.7 ± 0.24 MJ/m²/day, respectively. These high values suggest significant potential for solar power generation in the region, which currently lacks sufficient clean energy. Factors like weather, topography, and local conditions influence solar radiation levels. Dhankutta's favorable conditions, including low pollution and cloud cover, contribute to its high solar insolation, making it an ideal location for solar energy development. Due to its superior performance, the CD model, evaluated alongside three others using RadEst 3.0, proved most suitable for this hilly region. The model's coefficients can be applied to estimate solar radiation and energy in similar areas of Nepal.

ACKNOWLEDGMENTS

We thank FAOSDRN Agrometeorology Group, ISCI-Crop Science, and the Department of Hydrology and Meteorology for providing RadEst 3.0 software, manuals, and meteorological data, respectively. We also express gratitude to everyone who contributed to this study.

EDITOR'S NOTE

This manuscript was rigorously peer-reviewed and subsequently accepted for inclusion in the special issue of the Journal of Nepal Physical Society (JNPS) after it was submitted to the Association of Nepali Physicists in America (ANPA) Conference 2024.

REFERENCES

1. Shrestha JN, Bajracharya TR, Shakya SR, Giri B. Renewable energy in Nepal-progress at a glance from 1998 to 2003. Inproceedings of the international conference on renewable energy technology for rural development (RETRUD-03) 2003 Oct (Vol. 3, pp. 12-14).

2. Ali MA, Elsayed A, Elkabani I, Akrami M, Youssef ME, Hassan GE. Optimizing artificial neural networks for the accurate prediction of global solar radiation: A performance comparison with conventional methods. energies. 2023 Aug 24;16(17):6165.

3. Teyabeen AA, Elhatmi NB, Essnid AA, Mohamed F. Estimation of monthly global solar radiation over twelve major cities of Libya. Energy and Built Environment. 2024 Feb 1;5(1):46-57.

4. Narejo KA, Rehman SU, Tariq I, Zahid MM, Sadiq N, Khan MM, Uddin Z. MEP modelled new equations for ASHRAE constant to estimate solar radiation. Indian Journal of Physics. 2024 Feb 22:1-5.

5. Poudyal KN. *Estimation of global solar radiation potential in Nepal* (Doctoral dissertation).

6. Joshi U, Poudyal KN, Karki IB, Chapagain NP. Evaluation of global solar radiation using sunshine hour, temperature and relative humidity at low land region of Nepal. Journal of Nepal Physical Society. 2020 Aug 2;6(1):16-24.

7. Joshi U, Karki IB, Chapagain NP, Poudyal KN. Prediction of daily global solar radiation using different empirical models on the basis of meteorological parameters at Trans Himalaya Region, Nepal. Nepal BIBECHANA. 2021 Jan 1;18(1):159-69.

8. Dhakal S, Gautam Y, Bhattarai A. Evaluation of Temperature-Based Empirical Models and Machine Learning Techniques to Estimate Daily Global Solar Radiation at Biratnagar Airport, Nepal. Advances in Meteorology. 2020; 2020(1): 8895311.

9. Joshi U, Chapagain NP, Karki IB, Shrestha PM, Poudyal KN. Estimation of daily solar radiation flux at Western Highland, Simikot, Nepal using RadEst 3.0 software. International Journal of System Assurance Engineering and Management. 2022 Feb;13(1):318-27.

10. Poudyal KN, Bhattarai BK, Sapkota B, Kjeldstad B, Daponte P. Estimation of the daily global solar radiation; Nepal experience. Measurement. 2013 Jul 1;46(6):1807-17.

11. Poudyal KN, Bhattarai BK, Sapkota B, Kjeldstad B. Estimation of the daily global solar radiation using RadEst 3.00 software-a case study at low land plain region of Nepal. Journal of Nepal Chemical Society. 2012; 29:48-57.

12. Khatri Chhetri BR, Gurung S. Estimation of total solar radiation using RadEst 3.00 software at Jumla, Nepal. International Journal of System Assurance Engineering and Management. 2017 Nov; 8:1527-33.

13. Bristow KL, Campbell GS. On the relationship between incoming solar radiation and daily maximum and minimum temperature. Agricultural and forest meteorology. 1984 May 1;31(2):159-66.

14. Donatelli M, Campbell CS. A simple model to estimate global solar radiation. InProc. of the 5th ESA Congress-Nitra, The Slovak Republic 1998 (pp. 133-134).

15. Donatelli M, Bellocchi G. Estimate of daily global solar radiation: new developments in the software RadEst3. 00. InProceedings of the 2nd International Symposium on Modelling Cropping Systems, Florence, Italy 2001 Jul 16 (pp. 16-18).

16. Donatelli M, Bellocchi G, Fontana F. RadEst3. 00: software to estimate daily radiation data from commonly available meteorological variables. European Journal of Agronomy. 2003 Jan 1;18(3-4):363-7.

17. Joshi U, Chapagain NP, Karki IB, Shrestha PM, Poudyal KN. Estimation of daily solar radiation flux at Western Highland, Simikot, Nepal using RadEst 3.0 software. International Journal of System Assurance Engineering and Management. 2022 Feb;13(1):318-27.